

imperturbable entity. This view appears to be compatible with all evidence from inorganic spectroscopy.

Both features—absence of a vacant  $t_{2g}$  orbital and strongly reduced J-T coupling—are closely connected to the half-filled shell character of these states. To the extent that a state is adequately described by a half-filled shell, it effectively protects itself against both reactive and nonreactive distortions.

**Acknowledgment.** We are indebted to the Belgian Government (Programmatie van het Wetenschapsbeleid). A.C. thanks the Belgian Science Foundation (N.F.W.O.) for a postdoctoral fellowship.

### Appendix

**Some Useful Properties of the Electron-Hole Exchange Operator.** (1) The one-determinant functions of the type  $D^e_k$  are eigenfunctions of  $\mathcal{S}_z$

$$\mathcal{S}_z D^e_k = M_s \hbar D^e_k \quad (1A)$$

Since  $M_S = 0$  for the closed shell, specified by the set  $\{1, 2, 3, \dots, r\}$ , the effect of  $\mathcal{P}$  on  $D^e_k$  leads to a determinant, which is again an eigenfunction of  $\mathcal{S}_z$ , but with eigenvalue  $-M_s \hbar$

$$\mathcal{S}_z \mathcal{P} D^e_k = -M_s \hbar \mathcal{P} D^e_k = -\mathcal{P} \mathcal{S}_z D^e_k \quad (2A)$$

and

$$\mathcal{S}_z \mathcal{P} + \mathcal{P} \mathcal{S}_z = 0$$

(2) The effect of the step operators can be described as follows:

$$\mathcal{S}^\pm D^e_k = \sum_{i=1}^{r/2} (\dots s_\pm k_i \dots) = \sum_i c_i (\dots (k_i \mp 1) \dots) \quad (3A)$$

In this equation, it is assumed that the standard order of the spin orbitals is used throughout:  $\phi_\alpha$  always immediately precedes  $\phi_\beta$  (where  $\phi$  is an arbitrary space orbital of the set). The coefficient  $c_i$  is only different from zero if  $k_i$  corresponds to an unmatched  $\alpha$  or  $\beta$  spin, that is, if either  $\phi_\alpha$  or  $\phi_\beta$  belongs to  $k$ , but not both; therefore, if the orbitals in  $D^e_k$  are in standard order, so will the orbitals be in all the determinants of eq 3A.

$$\begin{aligned} \mathcal{P} \mathcal{S}^\pm D^e_k &= \sum_i c_i \mathcal{P} (k_1 \dots (k_i \mp 1) \dots k_n) \\ &= \sum_i c_i (-1)^{q_k \pm 1} (k_{n+1} \dots k_i \dots k_r) \\ &= -\sum_i c_i (-1)^{q_k} (k_{n+1} \dots k_i \dots k_r) \end{aligned}$$

The latter determinants are all characterized by  $(-M_S \mp 1)$ . They

differ from  $\mathcal{P} D^e_k(M_S) = D^h_k(-M_S)$  only in sign and in one spin orbital; they all have  $k_i$  rather than  $k_i \mp 1$  in  $D^h_k$ . Therefore

$$\begin{aligned} \mathcal{P} \mathcal{S}^\pm D^e_k &= -(-1)^{q_k} \sum_i c_i (k_{n+1} \dots k_i \dots k_r) \\ &= -(-1)^{q_k} \mathcal{S}^\mp (k_{n+1} \dots k_i \mp 1 \dots k_r) \\ &= -\mathcal{S}^\mp \mathcal{P} D^e_k \end{aligned} \quad (4A)$$

and

$$\mathcal{P} \mathcal{S}^\pm + \mathcal{S}^\mp \mathcal{P} = 0$$

(3) Since

$$\mathcal{S}^2 = \mathcal{S}_z^2 + 1/2(\mathcal{S}^+ \mathcal{S}^- + \mathcal{S}^- \mathcal{S}^+)$$

and

$$\begin{aligned} \mathcal{S}_z^2 \mathcal{P} &= -\mathcal{S}_z \mathcal{P} \mathcal{S}_z = \mathcal{P} \mathcal{S}_z^2 \\ \mathcal{S}^+ \mathcal{S}^- \mathcal{P} &= -\mathcal{S}^+ \mathcal{P} \mathcal{S}^+ = \mathcal{P} \mathcal{S}^- \mathcal{S}^+ \\ \mathcal{S}^- \mathcal{S}^+ \mathcal{P} &= -\mathcal{S}^- \mathcal{P} \mathcal{S}^- = \mathcal{P} \mathcal{S}^+ \mathcal{S}^- \end{aligned}$$

one obtains

$$\mathcal{P} \mathcal{S}^2 - \mathcal{S}^2 \mathcal{P} = 0 \quad (5A)$$

(4) If the labels  $\Gamma$ ,  $M_\Gamma$ , and  $S$  are known, specification of  $M_S$  completes  $K$  and eq 5 and eq 8 can be rewritten as

$$\mathcal{P} \Psi^e(M_S) = \Psi^h(-M_S) \quad (6A)$$

$$\Psi^h(M_S) = p \Psi^e(M_S) \quad (7A)$$

where  $p = \pm 1$ . Applying  $\mathcal{S}^\mp$  to eq 6A and using eq 4A, one obtains

$$\begin{aligned} \mathcal{S}^\mp \mathcal{P} \Psi^e(M_S) &= \mathcal{S}^\mp \Psi^h(-M_S) = -\mathcal{P} \mathcal{S}^\pm \Psi^e(M_S) = \\ &= -\mathcal{P} N \Psi^e(M_S \pm 1) = -N \Psi^h(-M_S \mp 1) \end{aligned}$$

where  $N$  is the positive constant appearing in the step operator. Clearly,

$$\mathcal{S}^\mp \Psi^h(-M_S) = -N \Psi^h(-M_S \mp 1)$$

Therefore, the step-operator constant is negative for the hole functions and positive for the electron functions. Since the number of steps between  $M_S$  and  $-M_S$  is a number with the same parity as the number of steps between  $M_S \pm 1$  and  $-M_S \mp 1$ , it follows from eq 7A that

$$\Psi^h(M_S \pm 1) = -p \Psi^e(M_S \pm 1)$$

Registry No. Cr<sup>3+</sup>, 16065-83-1.

## Structure of Glycolic Acid Determined by Microwave Spectroscopy

C. E. Blom and A. Bauder\*

Contribution from the Laboratory for Physical Chemistry, Swiss Federal Institute of Technology, CH-8092 Zurich, Switzerland. Received September 22, 1981

**Abstract:** The microwave spectra of all singly substituted D, <sup>13</sup>C, and <sup>18</sup>O species and one doubly substituted species of glycolic acid (CH<sub>2</sub>OHCOOH) have been measured and analyzed. From the moments of inertia of all species the complete molecular structure was determined. It shows an intramolecular hydrogen bond in which the hydroxyl group points toward the carbonyl oxygen of the carboxylic group with an O...H distance of 2.11 Å. The structure of the free molecule in the gas phase differs largely from the molecular structure in the crystal due to strong intermolecular hydrogen bonding in the solid state.

### Introduction

Glycolic acid (CH<sub>2</sub>OHCOOH) is the simplest member of the  $\alpha$ -hydroxycarboxylic acid series, which is of considerable biological

importance. Hydrogen bonding is crucial for the actual conformation of glycolic acid. In the solid state the conformation is dominated by two strong intermolecular hydrogen bonds to

Table I. Rotational Constants (MHz) and Inertial Defects ( $\text{u } \text{\AA}^2$ ) of the Isotopic Species of Glycolic Acid in the Vibrational Ground State<sup>a</sup>

species	$A^\circ$	$B^\circ$	$C^\circ$	$\Delta^\circ$ <sup>b</sup>	$n^c$
CH <sub>2</sub> OHCOOH	10696.0950 (24) <sup>d</sup>	4051.0323 (8)	2994.6632 (8)	-3.2422	85
CH <sub>2</sub> OH <sup>13</sup> COOH	10695.7310 (21)	4043.1721 (6)	2990.3393 (5)	-3.2423	30
<sup>13</sup> CH <sub>2</sub> OHCOOH	10565.6850 (31)	4033.4314 (9)	2974.8143 (8)	-3.2437	29
CH <sub>2</sub> OHCO <sup>18</sup> OH	10517.4110 (60)	3888.3322 (15)	2891.4293 (14)	-3.2397	23
CH <sub>2</sub> OHC <sup>18</sup> OOH	10018.3875 (32)	4035.1737 (12)	2930.5332 (11)	-3.2357	22
CH <sub>2</sub> <sup>18</sup> OHCOOH	10695.7526 (42)	3834.7553 (13)	2874.8073 (12)	-3.2438	28
CHDOHCOOH	10104.5619 (35)	4010.5025 (12)	2949.8740 (11)	-4.7066	74
CH <sub>2</sub> ODCOOH	10510.3526 (70)	3970.5866 (16)	2936.5264 (15)	-3.2637	24
CH <sub>2</sub> OHCOOD	10696.3321 (67)	3877.7275 (15)	2899.0324 (14)	-3.2497	26
CH <sub>2</sub> ODCOOD	10510.8985 (89)	3801.0417 (19)	2842.9092 (18)	-3.2712	25

<sup>a</sup> The frequencies for CH<sub>2</sub>OHCOOH and CHDOHCOOH were fitted by including all quartic centrifugal distortion constants (see Table II); the frequencies of the remaining species were fitted by taking over the quartic constants from the parent CH<sub>2</sub>OHCOOH. <sup>b</sup>  $\Delta^\circ = I_c^\circ - I_a^\circ - I_b^\circ$ . <sup>c</sup> Number of measured rotational transitions included in the least-squares fit. <sup>d</sup> The uncertainty is given in parentheses as one standard deviation.

neighboring molecules. This structure was determined by neutron<sup>1</sup> and X-ray<sup>2</sup> diffraction.

The free molecule might exist in more than one conformation depending on the relative strengths of different intramolecular hydrogen bonds. In a recent reinvestigation<sup>3</sup> of the microwave spectrum of glycolic acid reported earlier,<sup>4</sup> only one conformer could be detected. From the rotational constants,<sup>3,4</sup> the dipole components,<sup>3</sup> and quantum chemical calculations<sup>5</sup> it was concluded that the lowest conformer exhibits a planar skeleton with the hydroxyl group pointing toward the carbonyl oxygen of the carboxylic group. The intramolecular hydrogen bond thus forms a planar five-membered ring. Further support for the observation of a single conformer in the gas phase is coming from recent matrix infrared studies of glycolic acid performed in our laboratory.<sup>6</sup>

The results reported in this paper complete our investigations into the microwave spectrum of glycolic acid. Moments of inertia have been deduced from the rotational spectra of nine isotopic species. They allowed a complete determination of the molecular structure of glycolic acid despite the fact that three nuclei are located close to the *a* principal axis. The equations of Kraitchman as well as a least-squares method were used during the structure determination.

### Experimental Details

Samples containing a mixture of CH<sub>2</sub>OHCOOH, CH<sub>2</sub>ODCOOH, CH<sub>2</sub>OHCOOD, and CH<sub>2</sub>ODCOOD (each about 25 mol %) and a mixture of CH<sub>2</sub>OHCOOH, CH<sub>2</sub>OHC<sup>18</sup>OOH, CH<sub>2</sub>OHC<sup>18</sup>OH, and CH<sub>2</sub>OHC<sup>18</sup>O<sup>18</sup>OH (about 56, 19, 19, and 6 mol %, respectively) were synthesized by direct acid-catalyzed exchange of CH<sub>2</sub>OHCOOH with D<sub>2</sub>O and H<sub>2</sub><sup>18</sup>O, respectively. The samples of CH<sub>2</sub>OH<sup>13</sup>COOH and <sup>13</sup>CH<sub>2</sub>OHCOOH were prepared by base-catalyzed reaction with H<sub>2</sub>O from CH<sub>2</sub>Br<sup>13</sup>COOH and <sup>13</sup>CH<sub>2</sub>BrCOOH obtained commercially (Stohler Isotope Chemicals). The same reaction was used in order to obtain CH<sub>2</sub><sup>18</sup>OHCOOH from CH<sub>2</sub>BrCOOH and H<sub>2</sub><sup>18</sup>O. CHDOHCOOH was prepared by electrolytic reduction of glyoxylic acid in D<sub>2</sub>O followed by acid-catalyzed back-exchange of the acid and alcoholic deuterium with H<sub>2</sub>O. Further details on the preparation of the isotopic species of glycolic acid will be given elsewhere.<sup>6</sup>

The microwave spectrometers for recording the rotational spectra of glycolic acid have been described earlier.<sup>3</sup> Rotational transitions of isotopic species were predicted with the help of a model of the molecular structure from ab initio calculations<sup>5</sup> and the rotational constants of the parent species.<sup>3</sup> The  $J = 3 \leftarrow 2$   $\mu_a$  R-branch transitions could easily be assigned on the basis of their typical satellite pattern. R- and Q-branch transitions with higher *J* values were included later step by step.

### Analysis of Rotational Spectra

Rotational transitions of the parent isotopic species of glycolic acid were reported previously,<sup>3</sup> where transitions with  $J \leq 53$  were

(1) Ellison, R. D.; Johnson, C. K.; Levy, H. A. *Acta Crystallogr., Sect. B* **1971**, *B27*, 333.

(2) Pijper, W. P.; *Acta Crystallogr., Sect. B* **1971**, *B27*, 344.

(3) Blom, C. E.; Bauder, A. *Chem. Phys. Lett.* **1981**, *82*, 492.

(4) Scharpen, L. H. Abstracts of the 27th Symposium on Molecular Structure and Spectroscopy, Columbus, OH, 1972, E4, 77.

(5) Ha, T.-K.; Blom, C. E.; Günthard, Hs. H. *J. Mol. Struct. THEOCHEM* **1981**, *85*, 285.

(6) Hollenstein, H. et al., to be submitted for publication.

Table II. Centrifugal Distortion Constants Determined for the Ground State of CH<sub>2</sub>OHCOOH and CHDOHCOOH (in kHz)

	CH <sub>2</sub> OHCOOH	CHDOHCOOH
$\Delta J$	0.8162 (57) <sup>d</sup>	0.8059 (89)
$\Delta JK$	3.276 (29)	2.508 (45)
$\Delta K$	5.602 (96)	4.510 (136)
$\delta J$	0.2119 (15)	0.2155 (24)
$\delta K$	2.581 (40)	2.097 (58)
$n^a$	85	70
$J_{\text{max}}^b$	30	30
$\sigma$ , MHz <sup>c</sup>	0.033	0.042

<sup>a</sup> Number of measured rotational transitions included in the least-squares fit. <sup>b</sup> Highest value of *J* in the fit. <sup>c</sup> Mean residual error of a measured transition. <sup>d</sup> The uncertainty is given in parentheses as one standard deviation.

assigned. For all isotopic species 22–30 rotational transitions with  $J \leq 10$  were assigned and their frequencies measured except for CHDOHCOOH. A more extended search allowed the identification of 74 transitions with  $J \leq 30$  for this species. Tables with listings of all measured transition frequencies are available as supplementary material.

For the parent species<sup>3</sup> and the CHDOHCOOH species the three rotational constants and all five quartic centrifugal distortion constants were adjusted in a least-squares fit of the measured transition frequencies up to  $J \leq 30$ . The mean residual errors of 33 and 42 kHz of a measured transition frequency approach closely the estimated errors of 20 kHz of the frequency measurements. Systematic deviations from the neglect of higher order centrifugal distortion can be excluded completely.

Since only low-*J* transitions were assigned for the remaining isotopic species, centrifugal distortion constants could not be adjusted reliably. Therefore, the distortion constants were taken from the parent species when the rotational constants were determined in the least-squares fit. Similarly small residual errors of 20–46 kHz were obtained for the isotopic species. The results for the rotational constants and the moments of inertia are collected in Table I for all isotopic species. The centrifugal distortion constants of the parent species and of the CHDOHCOOH species are listed in Table II. The centrifugal distortion constants are defined with respect to Watson's asymmetric reduction in a prolate *I'* representation.<sup>7</sup>

### Molecular Structure

From the differences  $\Delta I_a^\circ$ ,  $\Delta I_b^\circ$ , and  $\Delta I_c^\circ$  between the moments of inertia in the vibrational ground state of the singly substituted species and the parent species all nuclear coordinates were calculated in the principal axes system of the parent molecule. Kraitchman's equations in three dimensions were used.<sup>8</sup> The results are given in Table III. The numbering of the nuclei is

(7) Watson, J. K. G. In "Vibrational Spectra and Structure"; Durig, J. R., Ed.; Elsevier: New York, 1977.

(8) Kraitchman, J. *Am. J. Phys.* **1953**, *21*, 17. Costain, C. C. *J. Chem. Phys.* **1958**, *29*, 864.

Table III. Cartesian Coordinates (Å) in the Principal Axes System of the Parent CH<sub>2</sub>OHCOOH Molecule, Obtained by Kraitchman's Method and by the Least-Squares Fit

nucleus	Kraitchman			least squares		
	<i>a</i>	<i>b</i>	<i>c</i>	<i>a</i>	<i>b</i>	<i>c</i>
C <sub>1</sub>	-0.4948	0.0396 (0.0738) <sup>a</sup>	±0.0077	-0.4964	0.0736	0.0
C <sub>2</sub>	0.7381	-0.7696	±0.0283	0.7374	-0.7704	0.0
O <sub>3</sub>	-1.6267	-0.6629	±0.0261 <sup>b</sup>	-1.6268	-0.6625	0.0
O <sub>4</sub>	-0.4923	1.2841	±0.0424 <sup>i</sup>	-0.4931	1.2837	0.0
O <sub>5</sub>	1.8981	0.0201 (0.0224) <sup>a</sup>	±0.0207	1.8981	0.0231	0.0
H <sub>6</sub>	0.7177	-1.4239	0.8802	0.7175	-1.4240	0.8803
H <sub>7</sub>	0.7177	-1.4239	-0.8802	0.7175	-1.4240	-0.8803
H <sub>8</sub>	1.5834	0.9256	±0.1060	1.5852	0.9263	0.0
H <sub>9</sub>	-2.3686	0.0722 <sup>i</sup>	±0.0631	-2.3687	-0.0084	0.0

<sup>a</sup> From the center of mass and the product of inertia conditions, with the assumption  $b(\text{H}_9) = -0.0084$  Å. <sup>b</sup>  $i = (-1)^{i/2}$ .

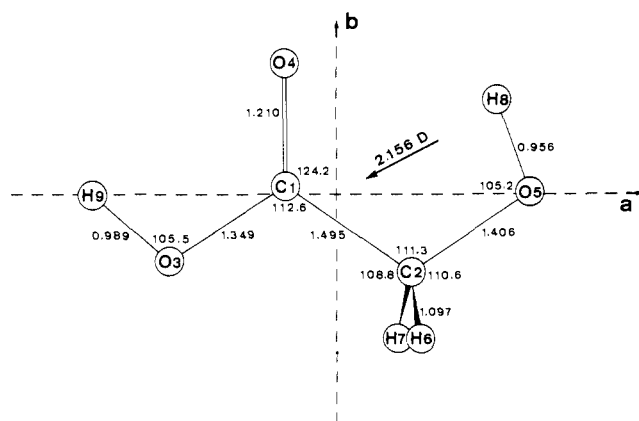


Figure 1. Glycolic acid: atomic numbering scheme, dipole moment, and structural parameters from the least-squares fit.

shown in Figure 1. Except for the hydrogen nuclei H<sub>6</sub> and H<sub>7</sub> the *c* coordinates of all other nuclei are small or even imaginary. They do not represent real deviations from positions in the symmetry plane but originate from vibrational effects neglected in the derivation of Kraitchman's equations.

Furthermore three of the *b* coordinates of the nuclei C<sub>1</sub>, O<sub>5</sub>, and H<sub>9</sub> are close to zero. Because they are so small, their accuracy suffers strongly from the neglect of systematic vibrational contributions. Therefore only the bond distances  $r(\text{C}_2\text{H}_6)$  and  $r(\text{C}_2\text{H}_7)$  and the bond angle  $\angle(\text{H}_6\text{C}_2\text{H}_7)$  are determinable accurately from the *r<sub>s</sub>* coordinates. In principle one can apply two additional conditions to the center of mass and the product of inertia in order to calculate coordinates of nuclei that are located too near a principal axis or that could not be substituted isotopically. However, this procedure does not suffice in the case of glycolic acid, where three nuclei are near the principal axis *a*.

A different approach was followed with our molecular structure program GEOM.<sup>9</sup> The differences  $\Delta I_a^\circ$ ,  $\Delta I_b^\circ$ , and  $\Delta I_c^\circ$  of the substituted species as well as the moments of inertia  $I_a^\circ$ ,  $I_b^\circ$ , and  $I_c^\circ$  of the parent molecule were considered to contain the structural information. The differences  $\Delta I_a^\circ$ ,  $\Delta I_b^\circ$ , and  $\Delta I_c^\circ$  for the doubly substituted CH<sub>2</sub>ODCOOH were also included. Bond lengths and bond angles of glycolic acid were adjusted directly in order to match observed and calculated data in a least-squares sense. The structure determined in this way automatically fulfils the center of mass and product of inertia conditions. The vibrational effects present in the moments of inertia even in the ground state cancel to the first order in the differences  $\Delta I_a^\circ$ ,  $\Delta I_b^\circ$ , and  $\Delta I_c^\circ$ . The differences were included in the least-squares fit with 100 times more weight than the moments of inertia of the parent molecule in order to compensate for the variations of estimated errors. The resulting bond lengths and bond angles are listed in Table IV. Residual errors of the differences after the least squares are smaller than 0.01 u Å<sup>2</sup> and those of the moments of inertia less than 0.7 u Å<sup>2</sup> (complete information is available as supplementary ma-

Table IV. Structural Parameters of Glycolic Acid

parameters	microwave	neutron
	least-squares	
	method	
	Lengths, Å	
C <sub>1</sub> -C <sub>2</sub>	1.495 (6) <sup>b</sup>	1.516 <sup>c</sup>
C <sub>1</sub> -O <sub>3</sub>	1.349 (6)	1.326
C <sub>1</sub> -O <sub>4</sub>	1.210 (6)	1.226
C <sub>2</sub> -O <sub>5</sub>	1.406 (4)	1.420
C <sub>2</sub> -H <sub>6,7</sub>	1.097 (3)	1.116
O <sub>3</sub> -H <sub>9</sub>	0.989 (19)	1.009
O <sub>5</sub> -H <sub>8</sub>	0.956 (3)	0.993
	Angles, Deg	
C <sub>2</sub> -C <sub>1</sub> -O <sub>3</sub>	112.6 (5)	112.1
C <sub>2</sub> -C <sub>1</sub> -O <sub>4</sub>	124.2 (4)	124.7
C <sub>1</sub> -C <sub>2</sub> -O <sub>5</sub>	111.3 (4)	112.2
C <sub>1</sub> -C <sub>2</sub> -H <sub>6,7</sub>	108.8 (3)	108.1
O <sub>3</sub> -C <sub>2</sub> -H <sub>6,7</sub>	110.6 (3)	108.7
C <sub>1</sub> -O <sub>3</sub> -H <sub>9</sub>	105.5 (11)	110.1
C <sub>2</sub> -O <sub>5</sub> -H <sub>8</sub>	105.2 (1)	109.8
	Torsional Angles, Deg	
H <sub>9</sub> O <sub>3</sub> C <sub>1</sub> O <sub>4</sub>	(0.0)	-3.5
O <sub>4</sub> C <sub>1</sub> C <sub>2</sub> O <sub>5</sub>	(0.0)	-1.3
C <sub>1</sub> C <sub>2</sub> O <sub>5</sub> H <sub>8</sub>	(0.0)	-79.7

<sup>a</sup> Reference 1. <sup>b</sup> The uncertainty is given in parentheses as one standard deviation. <sup>c</sup> Average value for the two independent molecules in the asymmetric unit cell. Bond lengths are corrected for thermal motion.

terial).

Cartesian coordinates in the principal axes system of the parent molecule are included in Table III. Comparison between substitution coordinates according to Kraitchman's equations and coordinates obtained with the least-squares method in Table III reveals a close agreement for the larger coordinates. However, the small *b* coordinates are shifted toward slightly larger values for the least-squares fit, as would be expected from considerations of the vibrational effects.

Among the three small *b* coordinates,  $b(\text{H}_9)$  contributes least to the center of mass and the product of inertia due to the small mass of hydrogen. Fixing  $b(\text{H}_9)$  at the least-squares value of  $-0.0084$  Å allowed the two remaining small *b* coordinates to be calculated from the center of mass and product of inertia condition by using only the large substitution coordinates. The results of  $b(\text{C}_1) = 0.0738$  Å and  $b(\text{O}_5) = 0.0224$  Å are very close to the least-squares coordinates in Table III. Variation of  $b(\text{H}_9)$  by 0.04 Å produces only small changes in  $b(\text{C}_1)$  of 0.006 Å and in  $b(\text{O}_5)$  of  $-0.002$  Å. This shows that these coordinates are reasonably determined from the two additional conditions. The small coordinate  $b(\text{H}_9)$  cannot be determined accurately. Its large uncertainty is reflected in the large standard deviations of the bond length O<sub>3</sub>-H<sub>9</sub> and the angle C<sub>1</sub>-O<sub>3</sub>-H<sub>9</sub> shown in Table IV from the least-squares fit.

The molecular structure of glycolic acid shown in Figure 1 results from the least-squares fit. The dipole moment is included in Figure 1 and was determined from Stark splittings.<sup>3</sup> The signs of the dipole components which are not accessible from Stark

(9) Nösberger, P.; Bauder, A.; Günthard, Hs. H. *Chem. Phys.* 1973, 1, 418.

splittings alone were chosen in order to be compatible with the ab initio results<sup>5</sup> and with model calculations from bond moments.

### Discussion

In Table IV the microwave gas-phase structure of glycolic acid is compared with the crystal structure from neutron diffraction determined by Ellison et al.<sup>1</sup>

Similar results were obtained by Pijper except that the positions of the hydrogen nuclei were less accurately determined from the X-ray diffraction.<sup>2</sup> Relatively large differences in the bond lengths of typically 0.02–0.03 Å in the bond angles up to 4.5° are observed between the gas-phase and solid-state structures. The differences may be traced back to extensive changes in the hydrogen bonding, i.e., intramolecular in the gas phase and intermolecular in the solid state. The skeleton of the heavy nuclei is still nearly planar in the crystal, but the torsion angle  $\tau$  ( $C_1C_2O_5H_8$ ) of the alcoholic hydroxyl group changes from 0° to –80° while forming one of the intermolecular hydrogen bonds. In the crystal, molecules are linked via strong short hydrogen bonds  $O_3-H_9\cdots O_5'$  of 1.64 Å and  $O_5-H_8\cdots O_4''$  of 1.76 Å. Apparently, this strong hydrogen bonding compensates for the deformations from the geometry of free glycolic acid, i.e., the breakage of the relatively weak intramo-

lecular hydrogen bond  $O_5-H_8\cdots O_4$  of 2.11 Å, the strain energy in the hydroxyl torsion, and the remaining deformations of the bond lengths and bond angles.

**Acknowledgment.** Financial support by the Swiss National Foundation (Project No. 2.612–0.80) is gratefully acknowledged. We thank N. Schwizgebel and G. Grassi for the preparation of isotopic species and Dr. H. Hollenstein for helpful discussions.

**Registry No.**  $CH_2OHCOOH$ , 79-14-1;  $CH_2OH^{13}COOH$ , 81277-96-5;  $^{13}CH_2OHCOOH$ , 81277-97-6;  $CH_2OHCO^{18}OH$ , 81277-98-7;  $CH_2OHC^{18}OOH$ , 81456-63-5;  $CH_2^{18}OHCOOH$ , 81277-99-8;  $CHDOHCOOH$ , 73654-45-2;  $CH_2ODCOOH$ , 81278-00-4;  $CH_2OHCOOD$ , 81278-01-5;  $CH_2ODCOOD$ , 81278-02-6.

**Supplementary Material Available:** Listings of measured rotational transition frequencies of  $CHDOHCOOH$ ,  $CH_2OH^{13}COOH$ ,  $^{13}CH_2OHCOOH$ ,  $CH_2OHCO^{18}OH$ ,  $CH_2OHC^{18}OOH$ ,  $CH_2^{18}OHCOOH$ ,  $CH_2ODCOOH$ ,  $CH_2OHCOOD$ , and  $CH_2ODCOOD$  in the vibrational ground state and least-squares fits of moments of inertia and shifts for glycolic acid and nine isotopic substituted species (Tables V–VII) (5 pages). Ordering information is given on any current masthead page.

## Visible Light Induced Water Cleavage in Colloidal Solutions of Chromium-Doped Titanium Dioxide Particles<sup>1a</sup>

Enrico Borgarello,<sup>1b</sup> John Kiwi,<sup>1b</sup> Michael Grätzel,<sup>\*1b</sup> Ezio Pelizzetti,<sup>1c</sup> and Mario Visca<sup>1d</sup>

Contribution from the Institut de Chimie Physique, Ecole Polytechnique Fédérale, CH-1015 Lausanne, Switzerland, the Istituto di Chimica Analitica, Università di Torino, Italy, and the Centro Ricerche SIBIT, Spinetta Marengo, Italy. Received October 13, 1981

**Abstract:** Surface doping of colloidal  $TiO_2$  particles with chromic ions precipitated from aqueous  $H_2SO_4$  solution produces very small ( $<0.1 \mu m$ ) mixed-oxide particles which absorb light in the 400–550-nm region in addition to the band-gap absorption of anatase. Sustained water cleavage by visible light is observed in aqueous solutions of these particles. Ultrafine deposits of Pt or  $RuO_2$  are necessary to promote water decomposition. A pronounced synergistic effect in catalytic activity is noted when both  $RuO_2$  and Pt are codeposited onto the particle. Wavelength dependency and kinetics of  $H_2$  and  $O_2$  evolution are examined.

Impurity doping is an important technique for improving the response of  $TiO_2$ -based photoelectrolysis cells.<sup>2–8</sup> While some dopants such as Be or Al ions increase the minority carrier diffusion length,<sup>4</sup> others such as Cr,<sup>2,3,5b,6,8,9</sup> Cd,<sup>4c</sup> or Co<sup>5a</sup> ions extend the spectral response of  $TiO_2$  into the visible by inducing optical transitions from d electrons of the metal to the  $TiO_2$  (or  $SrTiO_3$ ) conduction band. Chromium ions substituted for  $Ti^{4+}$  in the  $TiO_2$  lattice have so far yielded optimal results. However, the Cr centers in  $TiO_2$  have a low oscillator strength ( $\sim 10^{-4}$ ) which in view of the low solubility of Cr in this oxide (0.4 a/o) renders visible light

harvesting by these electrodes inefficient. Moreover, Cr affects adversely the photocurrent in the band-gap region of  $TiO_2$  due to a decrease in the hole diffusion length. At least for polycrystalline electrodes, this effect overcompensates the gain in overall conversion efficiency, which would be expected from the extension of the photoresponse towards the visible part of the spectrum.<sup>4c</sup>

In connection with our ongoing research on combined catalytic systems affording water cleavage by visible light,<sup>10–17</sup> we have performed extensive investigations with  $TiO_2$  particles loaded with ultrafine deposits of Pt and  $RuO_2$ .<sup>11–15,17</sup> During these experiments, it was discovered that direct band-gap excitation of the  $TiO_2$  sol

(1) (a) Presented in part at the Solar World Forum, Brighton, England, August 1981. (b) Institut de Chimie Physique. (c) Istituto di Chimica Analitica. (d) Centro Ricerche SIBIT.

(2) Ghosh, A. K.; Maruska, H. P. *J. Electrochem. Soc.* **1977**, *124*, 1516.

(3) Maruska, H. P.; Ghosh, A. K. *Sol. Energy Mater.* **1979**, *1*, 237.

(4) (a) Augustynski, J.; Hinden, J.; Stalder, C. *J. Electrochem. Soc.* **1977**, *124*, 1063. (b) Stalder, C.; Augustynski, J. *Ibid.* **1979**, *126*, 2007. (c) Monnier, A.; Augustynski, J. *Ibid.* **1980**, *127*, 1576.

(5) (a) Matsumoto, Y.; Kurimoto, J.; Amagasaki, Y.; Sato, E. *J. Electrochem. Soc.* **1980**, *127*, 2148. (b) Matsumoto, Y.; Kurimoto, J.; Shimizu, T.; Sato, E. *Ibid.* **1981**, *128*, 1040.

(6) Lampet, G.; Verniolle, J.; Doumère, J. P.; Claverie, J. *Mater. Res. Bull.* **1980**, *15*, 115.

(7) Goodenough, J. B. *Prog. Solid State Chem.* **1971**, *5*, 145–344.

(8) Mackor, A.; Blasse, G. *Chem. Phys. Lett.* **1981**, *77*, 6.

(9) Houlihan, J. F.; Armitage, D. B.; Hoovler, T.; Bonaquist, D.; Madacsi, D. P.; Mulay, L. N. *Mater. Res. Bull.* **1978**, *13*, 1205.

(10) Kalyanasundaram, K.; Grätzel, M. *Angew. Chem., Int. Ed. Engl.* **1979**, *18*, 701.

(11) Kiwi, J.; Borgarello, E.; Pelizzetti, E.; Visca, M.; Grätzel, M. *Angew. Chem., Int. Ed. Engl.* **1980**, *19*, 646.

(12) Grätzel, M. *Ber. Bunsenges. Phys. Chem.* **1980**, *84*, 981.

(13) Borgarello, E.; Kiwi, J.; Pelizzetti, E.; Visca, M.; Grätzel, M. *Nature (London)* **1981**, *284*, 158; *J. Am. Chem. Soc.* **1981**, *103*, 6423.

(14) Kalyanasundaram, K.; Grätzel, M. NATO Advanced Studies Treatise, NATO Summer School on Photoelectrochemistry, Gent, Belgium, 1980.

(15) Kalyanasundaram, K.; Borgarello, E.; Grätzel, M. *Helv. Chim. Acta* **1981**, *64*, 362.

(16) Duonghong, D.; Borgarello, E.; Grätzel, M. *J. Am. Chem. Soc.* **1981**, *103*, 4685.

(17) Grätzel, M. *Faraday Discuss. Chem. Soc.* **1980**, *70*, 359.